Assessment of pH stabilization in low temperature regions of long subsea pipelines

Attila PALENCSÁR[1], Marion SEIERSTEN[2], Tonje BERNTSEN [3, 4], Tor HEMMINGSEN[4]

[1] *Institute for Energy Technology (IFE), Kjeller, Norway, attila.palencsar@ife.no*
[2] *Institute for Energy Technology (IFE), Kjeller, Norway, marion.seiersten@ife.no*
[3] *Statoil ASA, Oslo, Norway, tber@statoil.com*
[4] *University of Stavanger, Stavanger, Norway, tor.hemmingsen@uis.no*

Abstract

Mitigation of CO_2 corrosion of carbon steel in oil and gas pipelines by pH stabilization is a well-established and proven approach with considerable benefits in terms of cost and environmental impact compared to the use of corrosion inhibitors. The essence of this technique is to employ strong alkalinity in order to promote formation of a protective iron carbonate layer on the carbon steel surface. As long as breakthrough of Ca-rich formation water is not expected, pH stabilization is a safe and reliable method that has been used in many fields with success.

During its development and qualification campaign the feasibility of pH stabilization was studied and proven experimentally for a wide range of relevant conditions, but not below 20 °C, particularly relevant for fields with cold subsea pipelines. While corrosion rates below 20 °C may in many cases be low, the low temperature corrosion behavior should not be disregarded without specific experimental trials. There can be scenarios where carbon steel corrodes at unacceptably high rates for a long enough time to exhaust the designed corrosion allowance.

Several experiments were conducted in the authors' laboratories, aimed at studying the corrosion and iron carbonate layer formation phenomena at lower temperatures. The results that are outlined in this paper show that around and under 20 °C protective iron carbonate film may take exceedingly long time to form or may not form at all within the timeframe of even long-term experiments; meanwhile the corrosion rates may remain above 0.1 mm/y. One reason for that can be that the corrosion mechanism in absence of film at high pH is not the same as at low pH.

The authors conclude that pH stabilization in colder subsea pipelines will, in most cases, still be feasible considering the inherently high pH this method implies as well as the presence of glycol, used to prevent hydrate formation. It should be emphasized that in order to ensure the integrity of the pipeline over its planned lifetime one must estimate the somewhat higher corrosion rate during a transient period and the corrosion rates after protection is obtained, and compare the accumulated material loss against the designed corrosion allowance. Alternatively, acceptably low corrosion rate without protection from $FeCO_3$ must be demonstrated. Both aspects must be tested experimentally and specifically for the actual pipeline conditions; corrosion models should not be used as the only benchmark for this purpose.

Introduction

Planning the exploitation of new oil and gas reserved always implies a careful assessment and balancing of investment costs and foreseen operational expenses. When it comes to corrosion mitigation of the transport pipelines this often means a choice to be made between corrosion resistant materials that carry a high investment cost or carbon steel that implies corrosion mitigation measures. Especially for long pipelines the feasibility of using carbon steel and corrosion control is always important to assess. Naturally, the savings on materials will only be justified if the corrosion mitigation approach is adequate considering the field conditions.

Mitigation of internal CO_2 corrosion of oil and gas transport pipelines typically involves creating a protective layer some kind on the inner pipeline surface that effectively reduces the corrosion rate. Without such a protective layer the corrosion rates may be considerably high and the corrosion allowance will be exhausted much sooner than the intended lifetime of the asset. Judicious selection and qualification of a corrosion mitigation approach can, on the other hand, effectively reduce corrosion rates. The two most established methods for CO_2 corrosion are the use of corrosion inhibitors and the pH stabilization technique. The examples shown in Figure 1 illustrate the possible outcome of unmitigated CO_2 corrosion compared to both pH stabilization and inhibition.

Inhibition is certainly the more widespread of these two methods due to the fact that it is in many cases applicable under circumstances that make pH stabilization unfeasible [1-3]. There are, however strong arguments to favor pH stabilization over inhibition when possible:

- It is more environment-friendly
- It is more cost-effective
- Has the added benefit of maintaining a very low dissolved ferrous ion concentration in the produced water, significantly reducing the potential of fouling of top side process equipment

pH stabilization is especially well suited to operations where glycols are used for hydrate prevention [2, 3]. This implies the presence of regions with low temperatures. During its development and qualification campaign the feasibility of pH stabilization was studied and proven experimentally for a wide range of relevant conditions, but mostly above 20 °C. While corrosion rates around and below 20 °C (particularly relevant for fields with cold subsea pipelines) may in many cases be low, the low temperature corrosion behavior should not be disregarded without specific experimental trials. There can be scenarios where carbon steel corrodes at unacceptably high rates for a long enough time to exhaust the designed corrosion allowance.

Experimental data from long-term tests relevant to this low-temperature scenario are scarce, likely due to the long duration such experiments require. The purpose of this paper is to review a series of published and yet unpublished experimental results obtained in the authors' laboratories that offer more insight into the time-scale of the development of protective iron carbonate layers around 20 °C along with an overview of key features of pH stabilization.

Figure 1   Comparison of carbon steel surfaces exposed to unmitigated CO_2 corrosion (upper image) and protected by inhibition (lower left) and pH stabilization (lower right)

The pH stabilization method

The use of pH stabilization is not a new concept; it was pioneered decades ago by Elf (now Total). Some of their experiences were described by Crolet et al. [4] and by Tobiassen et al. [5].

The merits of pH stabilization have been documented in the laboratory by extensive experimental campaigns carried out at IFE in Norway validating this approach for a wide range of conditions [2, 6]. There have also been numerous examples documenting successful application of this method over the past years. Statoil is operating a number of pH stabilized pipelines, most of them with hydroxide/carbonate as pH stabilizer. Several publications by Olsen et al. and Halvorsen et al. present both a comprehensive overview of the technique and experiences from fields in operation or under development [3, 7-10] citing no reports of corrosion failures in any of the fields. Table 1 shows an overview of fields where pH stabilization was implemented, based on information from the publications cited above [2, 3, 7].

Table 1:   Fields where pH stabilization has been applied. Based on references[2, 3, 7]

| Pipeline	Diam. - Length	Year	pH stabilizer	Max. temp. °C	Max. pCO$_2$ MPa	Max. pH$_2$S MPa
Italiana Mineraria (Elf)	10in - 12 km	1973	MBTNa + inh.	50	.17	0
Petroland (Elf)		1979	MBTNa + inh.	75	.07- .31	0
Pecorade, glycol contactor (Elf)		1982	MBTNa		9 %	15%
Heimdal MEG loop (Hydro)		1987	MDEA	40	.03-.04	0
Lille Frigg (Elf)	10in - 21 km	1994	MDEA	90	1	0
Frøy Gass (Elf)	12in - 32 km	1995	MDEA	30	.09	0
Troll-Kollsnes (Statoil)	36in - 66 km	1997	NaHCO$_3$	50	.04	0
Mensa (Shell)	12in - 97 km	1997	MEA	60	0.35	0
Huldra_Heimdal (Statoil)	20in - 150 km	2001	Alkylamine	50	0.4	0
Åsgard A-B (Statoil)	12in - 5.4 km	2001	NaHCO$_3$		>0.1	0
Midgard	20in - 40 km	2001	NaHCO$_3$ + inh.			
South Pars (Total)		2002	MDEA		>0.1	>0.05
Tune/Oseberg	12in - 11 km	2002	K$_2$CO$_3$ + inh.	100	0.7	
Vale	8in - 16 km	2002	K$_2$CO$_3$ + inh.	80	0.7	
Skirne/Bygve-Heimal (Total/Statoil)			Alkylamine	<50		
Goldeneye (Shell)	20in - 100 km	2004	NaOH/NaHCO$_3$	40	.037	0
Two Flow lines (Maersk)		2004	NaOH/NaHCO$_3$			
Kvitebjørn (Statoil)	30in - 147 km	2005	NaOH/NaHCO$_3$	55	0.2	<0.002
Visund (Statoil)	20in - 34 km	2005	NaOH			
Ormen Lange	30in - 120 km	2007	KOH + inhibitor.	85	0.11	
Snøhvit (Statoil)	28in - 144 km	2008	NaOH/NaHCO$_3$	75	0.5	0

The method of pH stabilization [2, 11] relies on injecting adequate amounts of strong alkalinity (denoted as pH stabilizer) to stimulate the formation of a protective iron carbonate layer on the corroding steel surface. This implies an increase the pH and generation of bicarbonate by reaction with carbonic acid resulting from dissolved CO$_2$ and water.

Taking the strong base KOH as an example, the sequence of relevant reactions will be as follows:
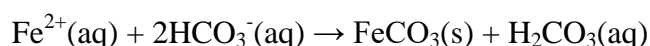
-   Dissolution/hydration of CO$_2$ generating carbonic acid

$$CO_2(aq) + H_2O \rightarrow H_2CO_3$$
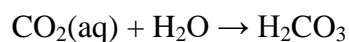
-   The strong base reacts with carbonic acid to form bicarbonate

$$KOH + H_2CO_3 \rightarrow KHCO_3 + H_2O$$
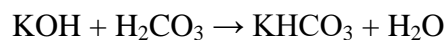
-   Increasing bicarbonate concentration promotes the formation of iron carbonate films as bicarbonate reacts with the divalent iron ions formed by corrosion:

$$Fe^{2+}(aq) + 2HCO_3^-(aq) \rightarrow FeCO_3(s) + H_2CO_3(aq)$$

The injected pH stabilizer is progressively diluted downstream the injection point by condensed water. Temperature and pressure also typically decrease along the pipeline resulting in increased solubility of FeCO$_3$. These changes result in progressively less favorable conditions for FeCO$_3$ precipitation downstream the pipeline. In order to obtain the

desired effects of pH stabilization, i.e. a protective iron carbonate layer, the concentration of bicarbonate must be sufficient to maintain a low $FeCO_3$ solubility in the colder regions of the pipeline, even at quite low Fe^{2+} concentrations. Figure 2 shows examples of protective iron carbonate layers formed on carbon steel.
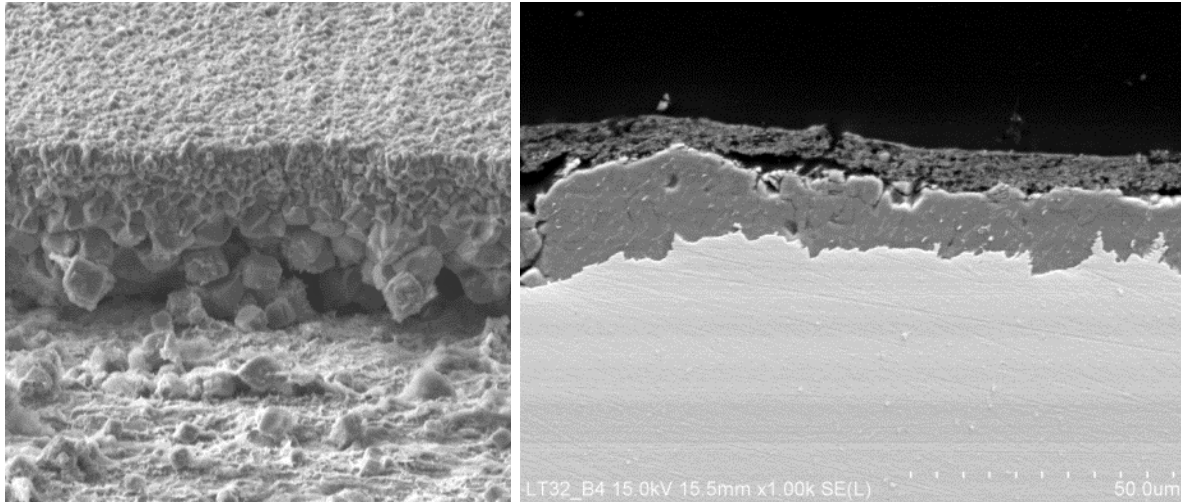

Figure 2   Perspective (left) and cross-section view (right) of protective iron carbonate layers formed under pH stabilized conditions.

It has to be noted that the presence of strong alkalinity renders this mitigation strategy incompatible with the production of formation water that often contains high levels of Ca^{2+}, carrying the risk of $CaCO_3$ scaling that could lead to the blocking of the pipeline [2, 10]. In many cases applying lower concentrations of alkalinity in combination with inhibitors can be viable up to certain levels of formation water ingress while providing some of the benefits of higher pH such as decreased baseline corrosion rate (i.e. assisting the inhibition) and low levels of dissolved iron. This is often referred to as partial pH stabilization or pH adjustment [3, 10].

The corrosivity of the system, i.e. the CO_2 partial pressure and temperature, determines largely the amount of base to be added: the higher the CO_2 partial pressure, the higher the required base concentration. The alkalinity requirement is calculated based on the thermodynamic solubility of $FeCO_3$ considering a target Fe^{2+} solubility selected as a function of the partial pressure of CO_2.

The formation of a protective iron carbonate film by employing pH-stabilization has been experimentally verified [6] in glycol solutions for temperatures as low as 20 °C. It is normally assumed that at lower temperatures a protective iron carbonate film will take either very long time to form or will not form at all, but even in the absence of such a film the corrosion rates will be acceptably low due to the low temperature and high pH. There are several CO_2 corrosion prediction models available [12] that can aid in this type of assessment, but caution must be exercised [13]. Particularly for the case of pH stabilization:

-   the in situ pH may often be beyond the range of such models
-   the effect of protective carbonate layers is practically impossible to quantify
-   quite importantly: the time frame in which protection is obtained cannot be predicted

Experimental

The results presented herein were obtained in experiments carried out either in one of IFE's flow loops or in a glass cell setup. Some of the data have been published earlier together with detailed accounts of the experimental details by Dugstad et al. [6] and Berntsen et al. [14]; only a brief description and relevant aspects are therefore included here.

The loop system (see a schematic diagram in Figure 3) is built of 316 L stainless steel and has two test sections that can be individually bypassed allowing removal of test sections independently without stopping the experiment. Test sections can house either tubular or flat specimens machined of the carbon steel to be tested. The specimens had electrical connections and were used as working electrodes for electrochemical LPR measurements. The steel specimens are held apart by insulating separators and flush mounted tightly inside the 316 L steel test sections; an illustration for tubular specimens is shown in Figure 3.
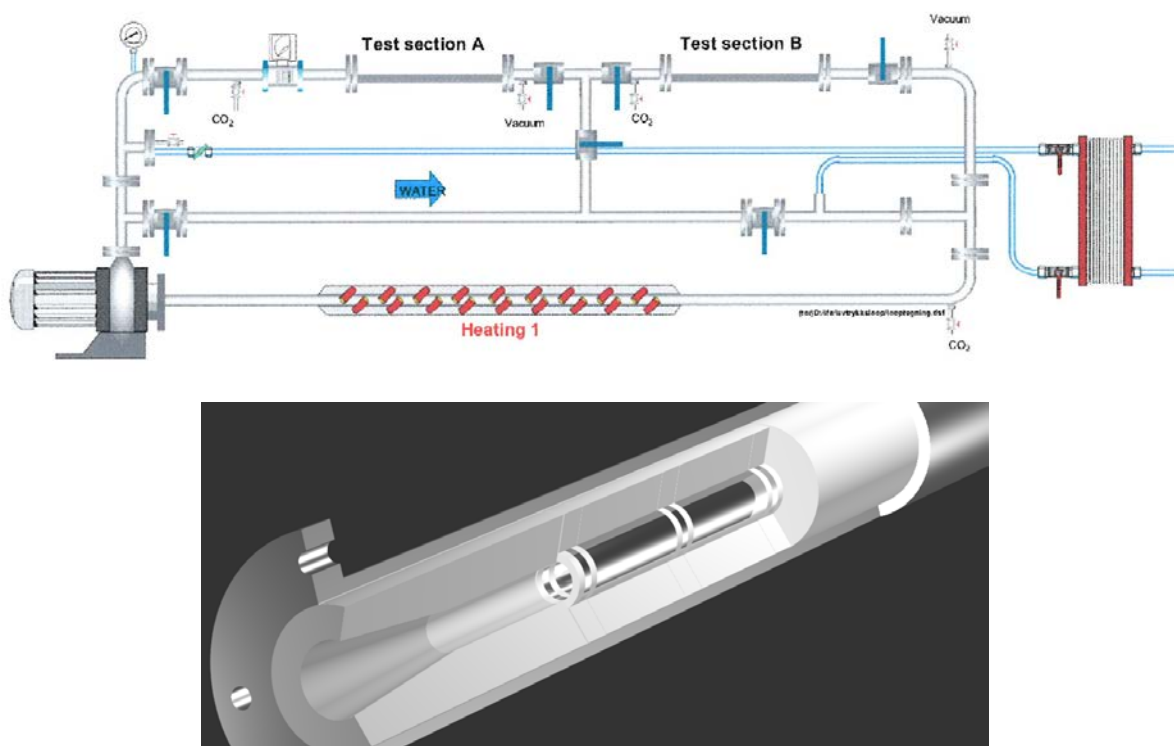
Figure 3   Upper panel: schematic drawing of IFE's low-pressure corrosion loop. Lower panel: perspective view of tubular carbon steel specimens mounted into the test section.

The glass cells used for corrosion testing have a 3L volume and are operated at atmospheric pressure with continuous purging. The cells are equipped with an air-tight lid with several feed-through fittings for auxiliary equipment (tubing, specimen holders, electrodes for electrochemical measurements) as shown in Figure 8.

Figure 4: Perspective drawing of a glass cell used for corrosion testing

The test brines are prepared from distilled water, technical grade glycol and technical grade chemicals as required. All test brines are carefully deaerated prior to experiments.

N_2 gas is used for deoxygenation, with an O_2-content below 1 ppm. The CO_2 gas used has a certified O_2-content below 5 ppm.

The carbon steel specimens are machined in-house. The specimens are cleaned with acetone in an ultrasonic bath, rinsed in ethanol and blow-dried before being mounted in the dry test sections or on the specimen holders.

During experiments the pH is continuously monitored. The Fe^{2+} content in the brine is measured on a regular basis from liquid samples using a photometric technique (absorbance at 508 nm after reaction with 1,10-Phenanthroline monohydrate producing an orange complex).

The corrosion rates are monitored using the Linear Polarization Resistance (LPR) technique, typically in a three-electrode configuration where each specimen acts as working electrode. The polarization resistance is used to calculate the corrosion current (and then the penetration or corrosion rate) using a Stern-Geary constant (also known as the "B" value) empirically set so as the average rates match the measured mass loss.

Post-exposure examinations are performed visually, by microscope and using a Scanning Electron Microscope (SEM) in top view and cross section.

Experimental data

A large part of the data from long-term pH stabilization experiments performed at lower temperatures originates from the experimental study/validation program carried out in the 1990's at IFE. Dugstad et al. presented a comprehensive report of the findings [6].

It was found that protective iron carbonate layers yielding acceptably low corrosion rates (i.e. below 0.1 mm/year) were easier to form in at temperatures within the 40-100 °C range, as shown in Figure 5. The same figure demonstrates that it proved to be more difficult to obtain protection at lower temperatures. When freshly abraded carbon steels were continuously exposed at 20 °C it took nearly four months to gain protection on St-35 steel whereas X65 and 0.5Cr steels continued to corrode at rates above 0.2 mm/y. Post-exposure examination revealed that iron carbonate layers have in fact started to form on the latter steel types as well.
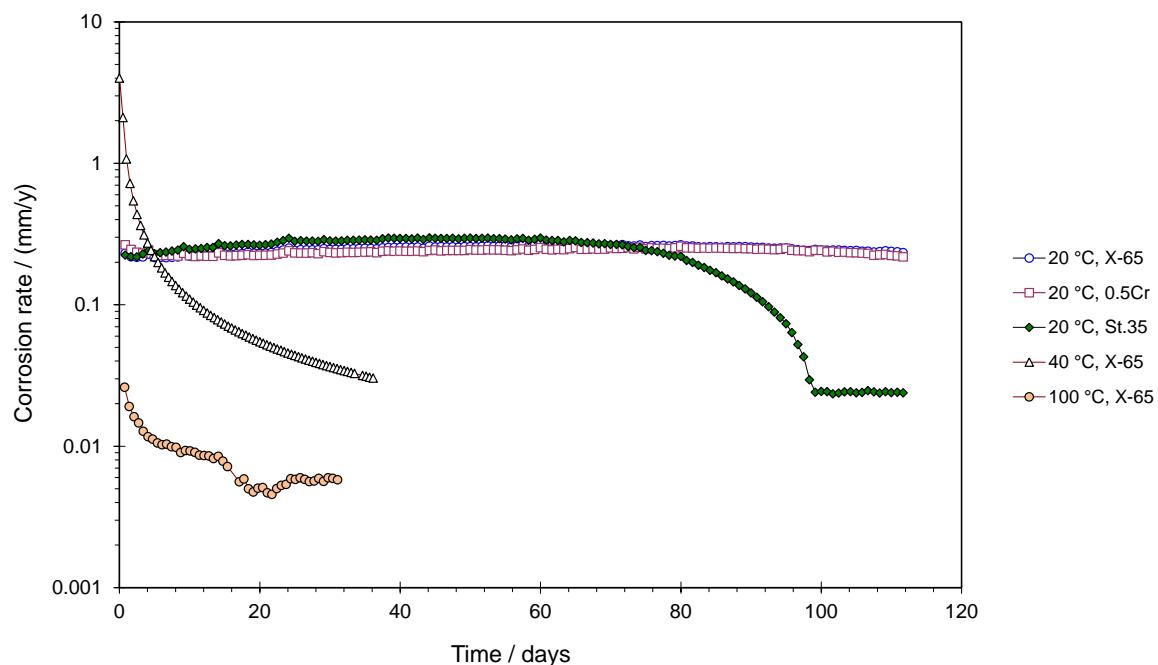
Figure 5   LPR corrosion rates of steel specimens at different temperatures (50 % DEG, 1 % NaCl, 6 bar CO_2, pH 6.5, flow 3 m/s). Adapted from Dugstad et al. [6] with permission.

It should be noted that the same experimental campaign also revealed a series of trigger factors that are highly relevant in the field and may facilitate obtaining protective layers under otherwise difficult conditions. Most interestingly, periods of stagnant or dry conditions as well as pre-existing surface oxides (e.g. a 20-30 µm thick magnetite layer) were shown to have beneficial effect. This implies that the condition of the inner surface of a pipeline (e.g. after rolling and storage) as well as common irregularities in operations (such as shut-down, draining of the pipeline and periodic oil coverage of the steel surface) can have a positive impact.

A long-term pH stabilization experiment at low temperature [14] was more recently performed using X65 carbon steel at ambient pressure (glass cell setup) with continuous purging of pure CO_2 yielding a partial pressure of ca. 1 bar and gentle stirring. This experiment was performed at room temperature, i.e. around 20 °C. One cylindrical specimen (1.0 cm high and 1.0 cm in diameter, used as the working electrode in the LPR measurements) and six flat, rectangular test coupons with a surface area of around 6 cm^2 were exposed in the test. The initial bicarbonate concentration was 22 mM, increased to 67 mM after a month.

A key feature of this experiment was the retrieval of one coupon each month, allowing the assessment of the development of iron carbonate layers in time.

The results of this experiment are shown in Figure 6. The initial corrosion rate was slightly below 0.2 mm/y and fairly stable. The increase of alkalinity concentration resulted in a drop in corrosion rate, followed, after several days by a continuous decrease to very low values (below 0.01 mm/y). In the same period the dissolved iron concentration reached a maximum after around 30 days and decreased to very low values again. These observations indicate that a protective iron carbonate layer has formed. More than two months' time was necessary for protection to be obtained under these conditions.
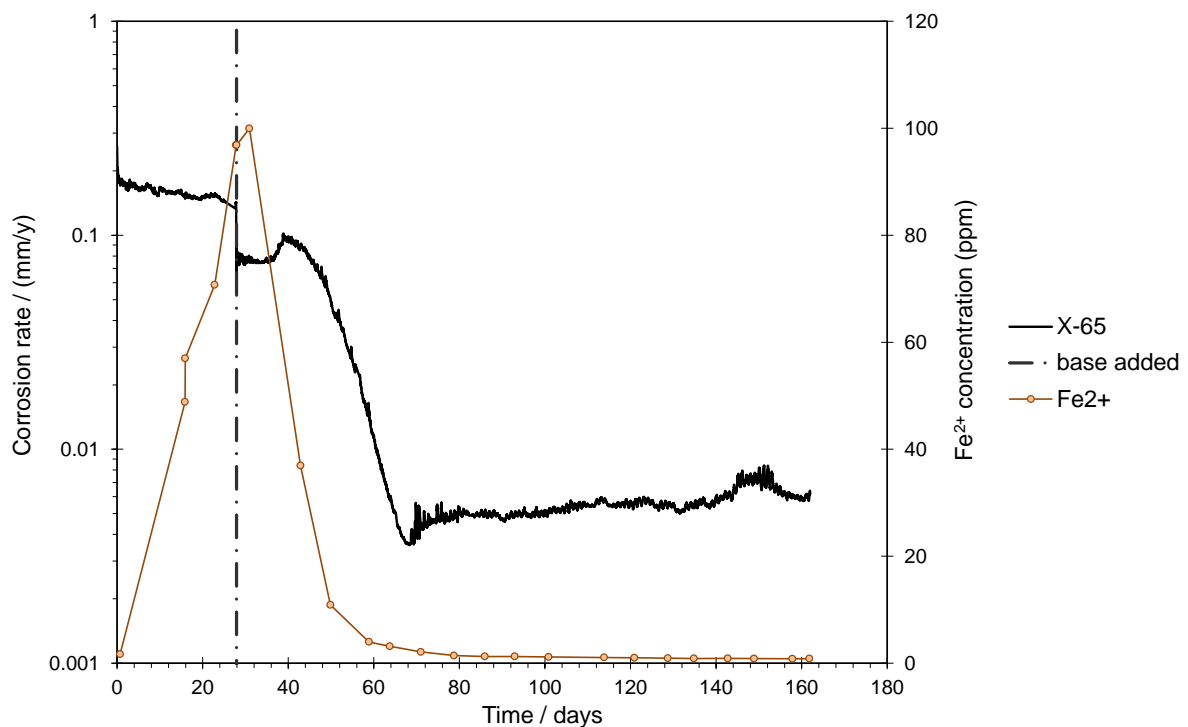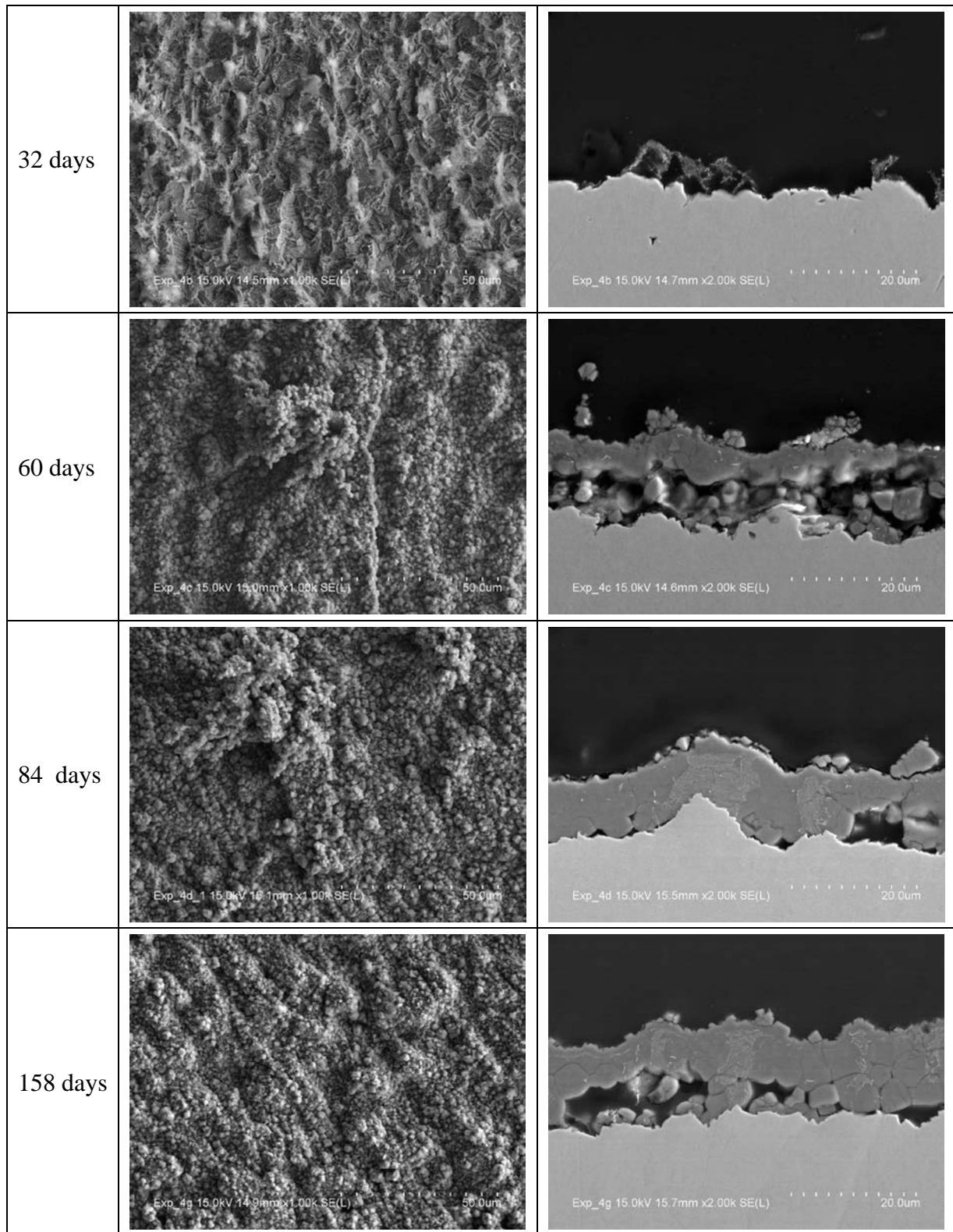

Figure 6   *LPR corrosion rate of X-65 steel specimen at room temperature (50 % MEG, 1 % NaCl, 1 bar CO$_2$). Adapted from Berntsen et al.[14] with permission.*

32 days		
60 days		
84 days		
158 days		

Figure 7   Surface and cross-section views of specimens from the long term experiment at room temperature (50 % MEG, 1 % NaCl, 1 bar CO_2). Adapted from Berntsen et al. [14] with permission.

Evaluation of the specimens retrieved after 32, 60, 84, 135, 158 and 162 days [14] give a fine illustration of the time-line of the iron carbonate development, as shown in Figure 7.

After 32 days no iron carbonate was observed, only exposed cementite. After 60 days (corrosion rate still decreasing) an FeCO3 layer is clearly established. By 84 and 158 days the layer became visibly more compact reaching a thickness of 10-15 μm. The film remained essentially unchanged and some voids were still observed after 162 days (not shown).

Another experiment, with flowing conditions was performed at 20 ºC after a 24 hour long precorrosion period at 60 ºC (applied in order to establish a uniformly corroding surface and thereby avoid artifacts). The test solution in this case consisted of 50 % MEG in water, 0.3 % NaCl. The CO_2 partial pressure was 3.2 bar and the flow 2 m/s through all the exposed tubular X65 carbon steel specimens. The pH stabilized conditions were obtained by adding ca. 150 mM MDEA reaching pH 6.8.

The evolution of the dissolved iron concentration was closely monitored together with the corrosion rates. When these indicated that a protective film was developing, one test section (two specimens) was removed for examination and the test continued with the remaining two specimens until protective film formation was considered complete.

The recorded corrosion rates are plotted vs. time in Figure 8. The measured dissolved iron concentration is also shown in the same graph.
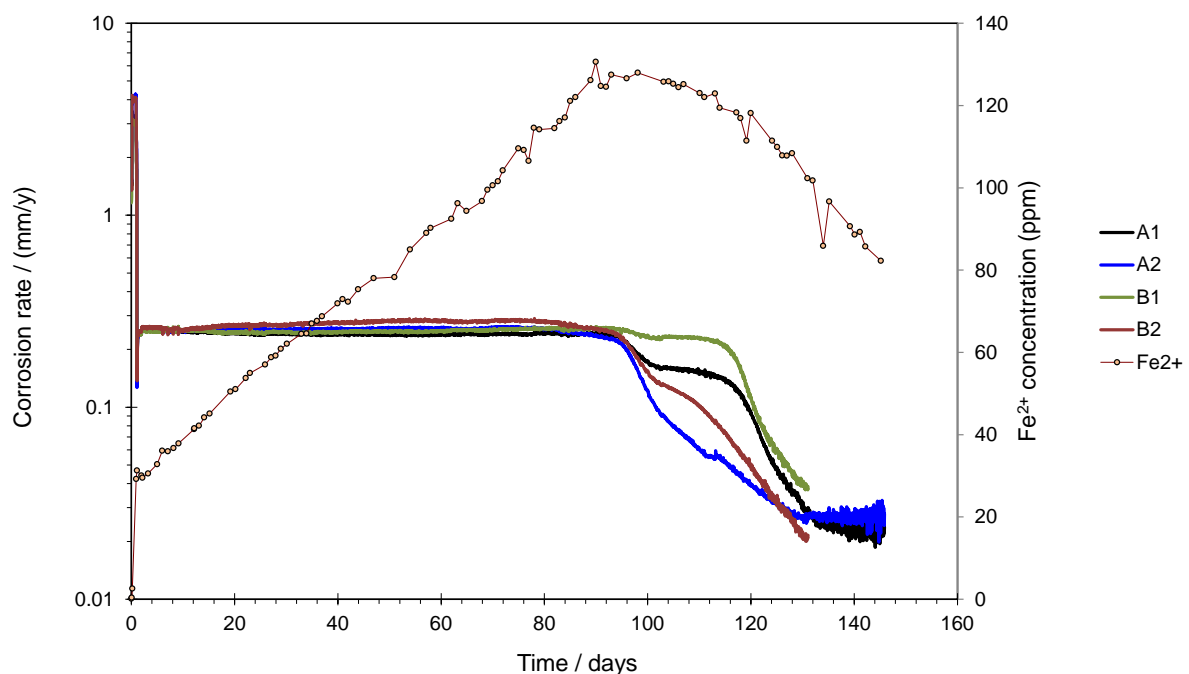

Figure 8   Plot of the corrosion rates (left axis) and ferrous ion concentration (right axis) recorded under pH stabilized conditions at 20 ºC (50 % MEG, 0.3 % NaCl, 3.2 bar CO_2, pH 6.8, flow 2 m/s)

In the precorrosion period (first ca. 24 hours, 60 °C) the corrosion rates were between 3-4 mm/y whereas the pH of the test solution was slightly increasing from below 4 to 4.6 due to the small amounts of alkalinity (bicarbonate) released by the corrosion process:

After precorrosion the temperature was allowed to decrease to the target 20 °C and the required amount of MDEA was injected (around the 31 hour mark). The pH increased accordingly, reaching a maximum value of 8.6 due to the consumption of the dissolved CO_2 (carbonic acid). The consumed CO_2 was gradually replenished by repeated additions until the reaction above was complete and the target CO_2 partial pressure was re-established and stable. The brine pH was 6.7 at this stage.

In the presence of the added alkalinity the corrosion rates of the four exposed specimens were around 0.25 mm/y for ca. 12 weeks. The steady increase in dissolved Fe^{2+} concentration also indicates a stable average corrosion rate of the same magnitude.

The increase in dissolved ferrous ion concentration started leveling off after ca. 90 days. Slight changes in the corrosion rate trends were also apparent. These are both signs that the overall rate of $FeCO_3$ precipitation reached a rate similar to that of iron dissolution by corrosion, and that at least some of the precipitated $FeCO_3$ was adhering to or growing on the exposed steel surfaces. The precipitation process became even more evident as the ferrous ion concentration started a decreasing trend.

The decrease in dissolved Fe^{2+} concentration was accompanied by an observable decrease of the corrosion rates, indicating that the carbon steel surfaces were being progressively covered by a developing $FeCO_3$ layer. It is interesting to note that within the period between 100 and 130 days the corrosion rates of the various specimens evolved differently. This may be due to the fact that initiation of film formation occurs randomly and the evolution of the surface coverage and hence protectiveness in time is not exactly the same for each specimen. The corrosion rates were converging again at the end of this period, suggesting that regardless of the differences in the development in time, the iron carbonate layers achieve similar quality and protectiveness once fully established. The Fe^{2+} concentration was still continuously decreasing, yet it seems that this (rather slow) precipitation process did not contribute significantly to the protectiveness at this stage. It is likely that prolonged exposure beyond this stage would lead to much lower dissolved iron concentration and increased robustness of the protective layers.

The final corrosion rates were on the order of 0.02-0.03 mm/y, i.e. an order of magnitude lower than those measured in the absence of a protective film under otherwise identical conditions.

Test section B was removed and the specimens inspected after 130 days, just prior to the corrosion rates leveling off to stable values. The iron carbonate layer on these specimens would be expected to be nearly, but not yet completely developed. Examination of the corroded surfaces supports this: as shown in the photographs of the inside surfaces of specimens B1 and B2 (see Figure 9), formation of corrosion product layers is quite evident even to the naked eye. It was interesting to find that on the surface of specimen B1 large areas of poorly adhering film had become dislodged, likely due to the flow during the experiment. In contrast, specimen B2 had its entire surface film largely intact with only blisters apparent. The appearance of specimen B1 is apparently in contrast with the degree of protection indicated by the electrochemical measurements. The explanation is provided by the SEM

images that show that a compact and nearly continuous layer adhering well to the steel surface exists underneath the poorly adhering one. As shown in Figure 10, the corrosion product film consists of three iron carbonate layers, also shown in higher magnification. The reason for such a morphology is rather unclear; one reason could be that the Fe^{2+} concentration greatly exceeds the solubility limit and therefore $FeCO_3$ nucleation and growth occurs both in the vicinity of the steel surface - near the source of additional Fe^{2+} - and from the bulk, eventually forming separate layers. The presence of the adherent film on the steel surface is important to note. This layer appears incomplete (voids with direct access to bare metal observable), which agrees well with the corrosion rates at the time of removal. The observations are also confirmed by the appearance of the surface layers viewed in cross section (see example in Figure 11).

Specimens A1 and A2 removed after the completion of the test (not shown) display very similar characteristics to B1 and B2, except that only two layers are apparent. No considerable areas of bare metal were observed. This is a clear indication of the completion of the protective film formation process.
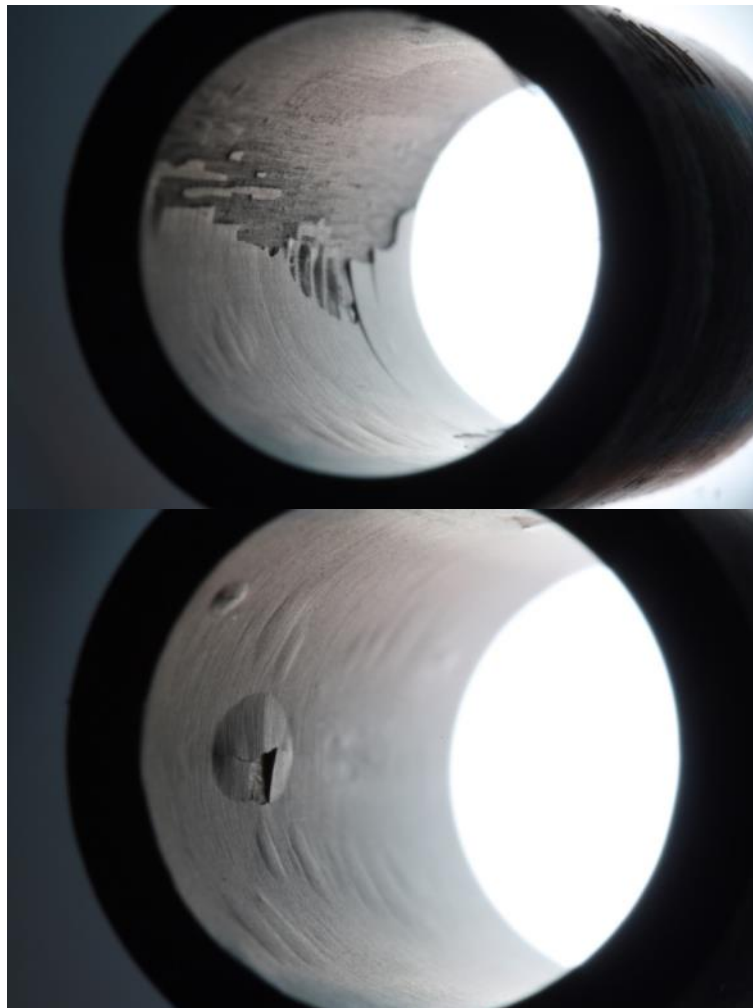
Figure 9   Photographs of the inside surface of specimen B1 (upper image) and B2 (lower image)
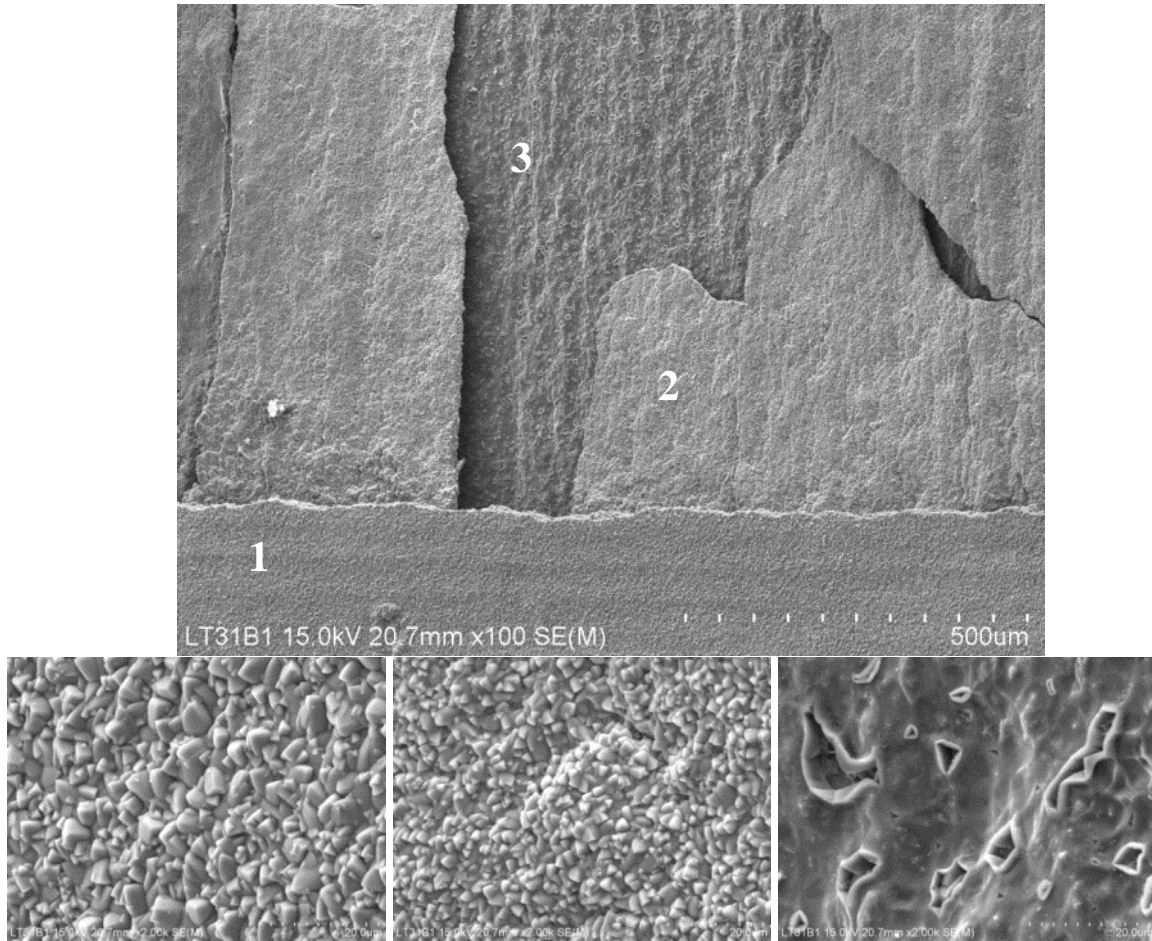
Figure 10   Upper image: top view SEM image from specimen B1. Lower images: Detail views of the regions labeled in as 1, 2 and 3.
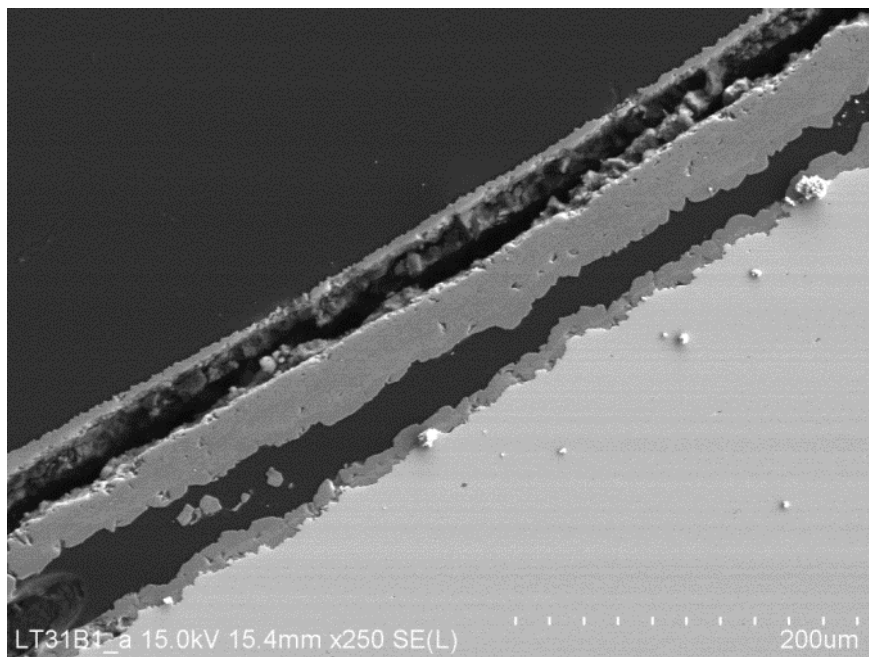
Figure 11   Cross section SEM image of specimen B1

Concluding remarks

The results obtained in the long-term pH-stabilization experiments demonstrate that protective iron carbonate films can in fact be formed at temperatures as low as 20 °C.

It is clear that at 20 °C the kinetics of the processes associated with protective film formation (i. e. nucleation and growth) are very sluggish. Under these conditions there may be very long periods of time with relatively high corrosion rates before the protective iron carbonate film is established.

The effect of even lower temperatures or lower CO_2 concentrations on film formation has yet to be experimentally investigated in detail. It can be anticipated that protective film would takes progressively longer to form as the temperature decreases further. This effect would be, to some degree, naturally offset by the decreasing corrosion rate during the time with no protection.

It is usually considered that at temperatures lower than 20 °C corrosion rates in the absence of a protective film, but benefiting from the presence of high levels of alkalinity would be acceptably low, therefore delayed or failed film formation may have little impact. The data reviewed here do not directly refute this view, but they suggest that, at least at relatively high CO_2 partial pressures, a gap may exist between safe conditions as a result of iron carbonate protectiveness and safe conditions as a result of low temperature where corrosion slows down significantly.

It can be speculated that the presence of pre-existing corrosion product or mill scale on the steel surface of a real pipeline or variations in operational conditions may have a positive effect on the establishment of a protective film compared to the freshly abraded specimens used in laboratory experiments. Such effects are, however, difficult to predict and should not be relied on as a certainty.

The results underline that the application of full pH-stabilization should always be very carefully assessed with respect to corrosion allowances. For any project based upon pH stabilization in low temperatures, the amount of metal loss which may occur prior to establishment of the protective film must be assessed, and an appropriate corrosion allowance added if necessary.

Many parameters affect the corrosion and iron carbonate formation processes in a complex way; it is quite difficult to predict the outcome under a given set of conditions with certainty. Model predictions are helpful, but conditions may often be outside the models range. In addition, the time to form a protective layer cannot be predicted.

It is therefore important that the corrosion rate without protection and the time it takes to obtain protection is tested experimentally and specifically for the actual pipeline conditions; corrosion models should not be used as the only benchmark for this purpose.

References

1. Palencsar, A. and Nyborg, R., *Experiences with Corrosion Inhibitor Testing at Elevated Temperatures*, Oil Field Chemistry Symposium, paper no. 16, Tekna, 2016.
2. Dugstad, A. and Seiersten, M., *pH-stabilisation, a Reliable Method for Corrosion Control of Wet Gas Pipelines*, paper no. SPE-87560-MS, Society of Petroleum Engineers, 2004.
3. Olsen, S. and Halvorsen, A. M. K., *Corrosion Control by pH Stabilization*, Corrosion 2015, paper no. NACE-2015-5733, NACE International, 2015.
4. Crolet, J.-L. and Samaran, J.-P., The use of the anti-hydrate treatment for the prevention of CO2 corrosion in long crude gas pipelines, National Association of Corrosion Engineers 1440 South Creek Dr., Houston, Texas 77084, USA, Houston (1993).
5. Tobiassen , P. and Pedersen, A. E., *Experience Feedback on the Use of a Carbon Steel Subsea Pipeline for a High Pressure, Sweet Service Gas Field*, Corrosion 2004, paper no. 04119, 2004.
6. Dugstad, A. and Dronen, P.-E., *Efficient Corrosion Control of Gas Condensate Pipelines by pH - Stabilization*, CORROSION 99, paper no. 99020, NACE International, 1999.
7. Olsen, S., *Corrosion Control by Inhibition, Environmental Aspects, and pH Control: Part II: Corrosion Control by pH Stabilization*, CORROSION 2006, paper no. 06683, NACE International, 2006.
8. Olsen, S., Lunde, O. and Dugstad, A., *pH-stabilization in the Troll Gas-Condensate Pipelines*, Corrosion 99, paper no. 99019, NACE International, 1999.
9. Hagerup, O. and Olsen, S., *Corrosion Control by pH Stabiliser, Materials and Corrosion Monitoring in a 160km Multiphase Offshore Pipeline*, Corrosion 2003, paper no. 03328, 2003.
10. Halvorsen, A. M. K., Andersen, T. R., Halvorsen, E. N., Kojen, G. P., Skar, J. I., Bjørnstad, C. and Fitje, H., *The Relationship between Internal Corrosion Control Method, Scale Control and MEG Handling of a Multiphase Carbon Steel Pipeline Carrying Wet Gas With CO_2 and Acetic Acid*, Corrosion 2007, paper no. 07313, NACE International, 2007.
11. Dugstad, A., *Mechanism of Protective Film Formation During CO_2 Corrosion of Carbon Steel*, Corrosion 1998, paper no. 98031, NACE International, 1998.
12. Nyborg, R., *Overview of CO_2 Corrosion Models for Wells and Pipelines*, Corrosion 2002, paper no. 02233, NACE International, 2002.
13. Olsen, S., *CO2 Corrosion Prediction by Use of the NORSOK M-506 Model - Guidelines and Limitations*, CORROSION 2003, paper no. 03623, NACE International, 2003.
14. Berntsen, T., Seiersten, M. and Hemmingsen, T., *Effect of $FeCO_3$ Supersaturation and Carbide Exposure on the CO_2 Corrosion Rate of Carbon Steel*, Corrosion, **69**, 601 (2013).